SSRG International Journal of Electrical and Electronics Engineering
ISSN: 2348-8379/ https://doi.org/10.14445/23488379/IJEEE-V13I4P105

Volume 13 Issue 4, 67-76, April 2026

Original Article

Modelling a Two-Phase Interleaved ZETA Converter using State-Space Representation

Mulchand Ayalani[1], Saurabh Pandya[2*]

[1]*Gujarat Technological University, Ahmedabad, India*
[2]*Electrical Engineering Department, Vishwakarma Government Engineering College, Chandkheda, Ahmedabad, India.*

[2]*Corresponding Author : saunipandya@rediffmail.com*

Received: 10 January 2026 Revised: 20 February 2026 Accepted: 20 March 2026 Published: 30 April 2026

Abstract *- In this paper, a comprehensive state-space modelling approach is developed for the dynamic analysis of a two-phase interleaved ZETA DC-DC converter operating in continuous conduction mode. The proposed approach systematically derives mode-wise differential equations, and the overall averaged state-space matrices of the converter are formulated. Using this model, the corresponding small-signal transfer function is derived analytically, enabling detailed analysis of the interleaved converter dynamics. The obtained model, described by differential equations, is implemented in the MATLAB environment to evaluate dynamic responses, including step, impulse, and frequency-domain characteristics. Simulation results in Simulink validate the accuracy of the formulated converter model. The developed model provides a control-oriented analytical foundation that can be effectively employed for closed-loop controller design in high-power DC-DC conversion applications.*

Keywords *- DC-DC converter, Interleaved ZETA (IZ) Converter, Modelling, State-Space Averaging (SSA) Model.*

1. Introduction

DC-DC converters are extensively used in modern industrial and commercial equipment such as electric vehicle battery chargers, power supplies, LED drivers, DC motor drives, renewable applications, etc. In power conversion systems, these converters have a pivotal role in regulating electrical power to obtain the desired voltage level, efficiency, and operational performance [1, 2]. Depending on application requirements, various DC-DC converter configurations have been introduced in literature to achieve step-up, step-down, or buck–boost voltage conversion [3, 4].

In recent applications of DC-DC converters, interleaved converter configurations have received significant attention for high-power applications, owing to their ability to reduce current ripple with improvement in converter efficiency, and enhance power-handling capability [5]. In particular, the interleaved ZETA (IZ) converter augments the benefits of ZETA converter topology with multiphase operation, enhancing improved dynamic characteristics and reduced stress on components.

An interleaved ZETA converter consists of multiple ZETA converter units connected in parallel, which are operating with 180° phase-shifted switching signals for a two-phase configuration. This approach results in reduced input and output current ripple [6, 7]. Although the state-space modelling technique of DC-DC converter topologies has been widely explored, detailed State Space Average (SSA) modelling and dynamic characterization of the interleaved ZETA converter have received limited attention in the literature. Most prevailing studies focus on circuit-level simulation or control implementation without explicitly deriving the averaged state-space matrices and small-signal transfer functions, which are essential for analysis of converter dynamics [8]. Consequently, a methodical analytical modelling approach is required to understand the dynamic behavior of the interleaved ZETA converter.

To address this gap, this study presents the state-space averaged modelling of a two-phase interleaved ZETA converter. It derives the corresponding dynamic equations and transfer function for system analysis.

The modelling procedure incorporates the derivation of mode-wise differential equations, the formulation of overall state-space averaged matrices [9], and dynamic response analysis for interleaved converter operation. Unlike several existing studies that primarily focus on simulation-based analysis [10], this study develops an analytical formulation of the averaged state space representation of the interleaved ZETA converter.

The key findings of this study are listed as follows:

- The complete SSA model of a two-phase interleaved ZETA converter is systematically derived, including

mode-wise differential equations and overall averaged matrices.
- Using the SSA model, the converter transfer function is obtained, allowing detailed analysis in both dynamic and frequency domains.
- The dynamic performance of the converter is investigated through step, impulse, and Bode responses under different duty-cycle conditions, establishing inherent system stability.

The proposed SSA analytical model is validated using MATLAB/Simulink simulations, providing a reliable framework for future closed-loop controller design.

The remainder of this study is divided into six sections. The literature review is included in section 2. The outline of the state-space averaging is discussed with the operation of the single-unit ZETA converter for reference in Section 3. In section 4, the modelling methodology using the state-space average technique of an interleaved ZETA converter is discussed based on the derivation of the differential equations. Section 5 discusses simulation results and dynamic analysis, while Section 6 concludes the study.

2. Literature Review

Various DC-DC converter configurations and their modelling methods have been explored in the literature. Conventional buck and boost converters are widely adopted for step-down and step-up applications, respectively. With appropriate circuit design and closed-loop control, the buck-boost converter can either raise or reduce the input voltage. The different converter topologies for extremely low voltage have been introduced in the literature, such as cascaded [11], quadratic [12, 13], multiphase [14], or hybrid step-down converters [15, 16], etc. However, applications demanding reduced current ripple, wide voltage conversion ratios, and better power density have led to the development of advanced converter configurations.

The steady state and dynamic behavior of conventional buck, boost, and buck–boost converters have been thoroughly examined in prior studies.

Interleaved basic converter topologies have also been investigated by researchers to improve system performance by reducing current ripple and enhancing efficiency. These configurations distribute power across multiple phases, with improved thermal characteristics and reduced stress on switching devices.

An accurate representation of DC-DC converter dynamics is essential for system analysis and controller design. Different modelling and simulation methods for DC-DC converter topologies have been investigated by researchers, including mathematical, circuit-based simulation, transfer function modelling, and state-space approaches. The circuit based modelling is the most common method, where the converter topology is drawn schematically in a modelling environment [17]. Mathematical modelling involves mathematical language/techniques to represent a system, providing insight into the behavior of the physical system. Among these, the state-space averaging approach has emerged as a powerful and widely accepted technique for developing control-oriented models for control applications of switching converters operating under Continuous Conduction Mode (CCM) [18, 19, 20].

Several studies have focused on the development of generalized state-space averaging models for different converter topologies. These models provide in-depth knowledge of system dynamics and assist controller design [21, 22]. However, most of these studies are limited to basic converter topologies and do not address the detailed modelling of the interleaved ZETA converter.

Additionally, current research often focuses on simulation-based analysis instead of developing analytical models for the analysis of the system's dynamic behavior. The lack of comprehensive SSA based modelling for IZ converters shows the need for a systematic approach to represent their behavior under different operating conditions.

3. Overview of State-Space Averaging Method

State-Space Averaging (SSA) serves as a mathematical approach for modelling and analyzing the dynamic response of switching converters. In this approach, the converter dynamics are represented using state variables, input variables, and output variables, described by first-order differential equations. Depending upon the power device's switching state, the circuit configuration of the converter working in continuous current mode changes within each switching time interval.

Over one switching cycle T, the converter operates in two modes. For an ON duration DT of the switch, the system behavior is described by one set of state equations. where D denotes the duty cycle of the converter's operation. A different set of state equations governs the converter's behavior during the interval $(1-D)T$, while the switch is OFF. An averaged state-space model is obtained by applying duty cycle-based weighting to the state equations corresponding to each switching interval. This averaged representation provides a continuous-time model that effectively captures the converter's low-frequency dynamic behavior and is particularly suitable for control-oriented analysis.

Further, a small-signal perturbation is applied to linearize the SSA model about its steady-state operation, enabling the derivation of transfer functions and frequency-domain characteristics. Due to its analytical clarity and suitability for

controller design, SSA has been extensively used for modelling converters operating in CCM.

3.1. State-Space Averaging Methodology

The state of the converter's operation in CCM depends upon the ON and OFF conditions of the power switch. The state-space equations for the two operating modes corresponding to each switching state are described as follows.

During the ON-state interval $0 < t < DT$, the converter's state equations can be written as:

$$\dot{x} = A_1 x(t) + B_1 u(t) \quad (1)$$

$$y(t) = C_{S1} x(t) + E_1 u(t) \quad (2)$$

Similarly, for the OFF-state interval ($DT < t < T$):

$$\dot{x} = A_2 x(t) + B_2 u(t) \quad (3)$$

$$y(t) = C_{S2} x(t) + E_2 u(t) \quad (4)$$

The resulting converter's SSA model for one switching period is modelled as:

$$\dot{x}_T(\mathrm{t}) = A_T x(t) + B_T u(t) \quad (5)$$

$$y_T(t) = C_{ST} x(t) + E_T u(t) \quad (6)$$

From Equations 5 and 6, the averaged state-space matrices can be obtained as:

$$\begin{cases} A_T = DA_1 + (1-D)A_2 \\ B_T = DB_1 + (1-D)B_2 \\ C_{ST} = DC_{S1} + (1-D)C_{S2} \\ E_T = DE_1 + (1-D)E_2 \end{cases} \quad (7)$$

- A_1, A_2, A_T = State matrix.
- B_1, B_2, B_T = Input matrix.
- C_{S1}, C_{S2}, C_{ST} = Output matrix.
- E_1, E_2, E_T = Feedforward (Direct Transfer) matrix.

This state-space averaged representation provides a continuous-time nonlinear model of the converter. Using a small signal perturbation about the steady state operating condition, the system response can be linearized to derive the transfer function from nonlinear Equations 5 and 6.

The steady-state expression can be derived using Equations 5 to 7, which results in:

$$\begin{cases} X = -{A_T}^{-1} B_T U \\ Y = (-C_{ST} {A_T}^{-1} B_T + E_T) U \end{cases} \quad (8)$$

3.2. Single ZETA Converter Configuration

The single-unit ZETA converter comprises power components (Switch-S and Diode-D), reactive elements (capacitors C_1, C_2, and inductors L_1, L_2), as illustrated in Figure 1. The converter can operate in both step-down and step-up modes while maintaining output voltage polarity. It is capable of providing an output voltage that may be lower, higher, or equal to the input voltage, supplying power to the load. In this topology, due to the presence of an inductor at the load side, the output current is mostly continuous. The input current may be discontinuous.

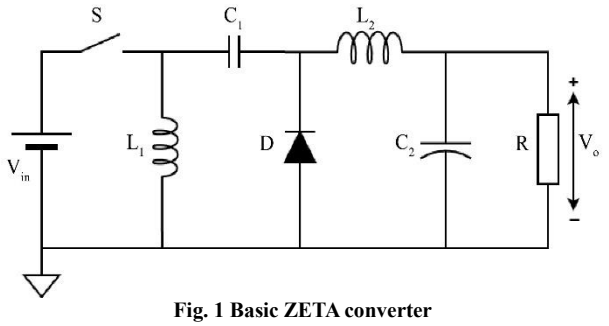

Fig. 1 Basic ZETA converter

3.3. Modes of the ZETA Converter

The converter's operation under CCM is divided into two states, as shown in Figure 2.

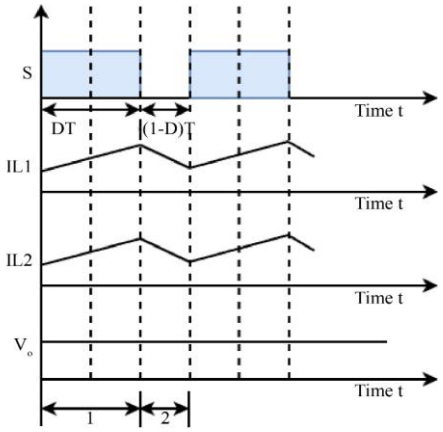

Fig. 2 Steady state waveforms of ZETA converter

3.3.1. State-1 Operation ($0 < t \leq DT$)

During this state, the switch S is ON. The source voltage V_{in} energizes the inductors. Hence, inductor currents i_{L1} and i_{L2} rise linearly, as shown in Figure 2. During this mode of operation, the inductors store energy, indicating that the converter is in the charging phase.

3.3.2. State-2 Operation ($DT < t \leq T$)

For the OFF state of the power switch S, the energy stored in the inductors L_1 and L_2 is released to the capacitors C_1 and C_2. As a result, the currents through inductors i_{L1} and i_{L2} decrease in a linear manner. This interval corresponds to the discharge mode, during which energy is supplied to the load.

In the SSA formulation, the inductor currents and capacitor voltages of the ZETA converter are considered as state variables, given by:

$$x(t) = [i_{L1}\ \ i_{L2}\ v_{C1}\ \ v_{C2}] \quad (9)$$

Using a set of differential equations, the state-space averaging model can be formulated for the ON and OFF states. From Equation 8, the converter's transfer function is derived by expressing the corresponding state space matrices. Further analysis of the converter's steady-state characteristics can be carried out.

4. State-Space Modelling of the Interleaved ZETA Converter

4.1. Circuit Description and Converter Parameters

The interleaved ZETA converter is suitable for high-power applications. This converter uses interleaved switching for ZETA converter topologies to achieve performance advantages. It has current sharing capability, which makes it suitable for parallel operation and redundant in power supply systems.

Figure 3 shows a circuit diagram of the non-isolated interleaved ZETA converter. This converter topology comprises two identical ZETA converter configurations that are interleaved and supply a load with phase-shifted switching signals. The circuit consists of power switches (S_1, S_2), upper phase inductors (L_{U1}, LU_2), diodes (D_1, D_2), lower phase inductors (L_{L1}, L_{L2}) and energy transfer capacitor (C_{U1}, C_{L1}). The common output capacitor C_2 and load R are connected at the output.

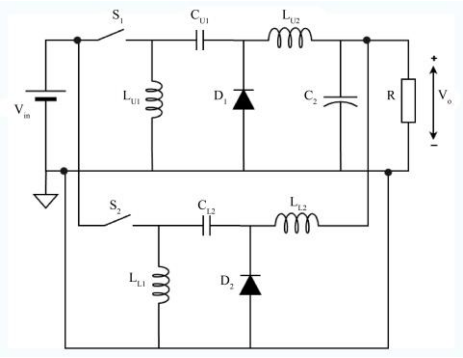

Fig. 3 Interleaved ZETA (IZ) converter

As per Table 1, the parameters of the interleaved ZETA converter are considered for modelling and simulation in the MATLAB environment.

Table 1. Specifications of IZ converter

Parameter	Value
Input Voltage Vin	200 Vdc
Inductance L_{U1}, L_{L1}	2 mH
Inductance L_{U2}, L_{L2}	1 mH
Capacitance C_{U1}, C_{L1}	220 uF
Capacitance C_2	15 uF
Switching frequency	50 kHz
Duty cycle *D*	Greater than 0.5
Load Resistance R	3 ohm

The interleaving technique shares current between phases, reducing input and output current ripple. Also, it enhances the power-handling capability of the converter, augmenting its suitability for high-power applications. The phases are operated with a phase shift of 180° at the same switching frequency.

4.2. Modes of the Interleaved ZETA Converter

The interleaved ZETA (IZ) converter's operation depends on the phase-shifted control signals of switches S_1 and S_2 and the duty cycle. The converter exhibits four distinct operating modes within one switching interval due to the overlap of conduction periods between the two phases for a duty cycle value greater than 0.5.

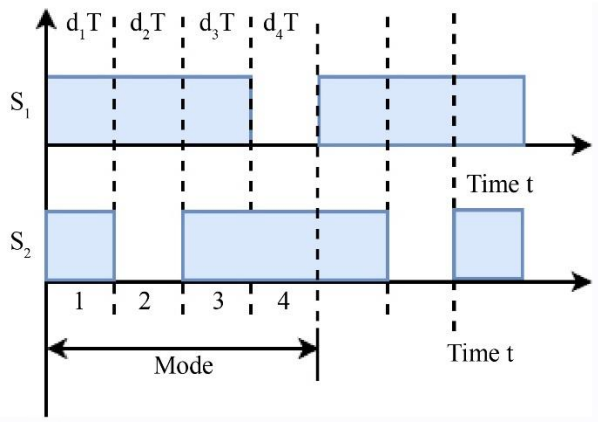

Fig. 4 Switching operation for duty cycle D > 0.5

The switching states of power devices S_1 and S_2 are illustrated in Figure 4, corresponding to each mode and the associated time intervals in fractions of the switching interval. The interleaved operation ensures that at least one phase actively transfers energy during each sub-interval, causing a reduction in current ripple and improving dynamic performance.

Likewise, for a duty cycle value less than *0.5*, at any given interval, the switching pattern of the power switches can be attained to examine the operation of an IZ converter, where only one power switch remains ON, and the other remains OFF during the overall switching period.

For converter operation, the state-space variables are deliberated as:

$$x(t) = [i_{LU1}\, i_{LU2}\, i_{LL1}\, i_{LL2}\, v_{CU1}\, v_{CL1}\, v_{C2}] \quad (10)$$

4.3. Operation in Mode 1 and Mode 3

For this operation, both power switches of the converter are in the ON state, whereas the diodes are reverse-biased. The corresponding circuit configuration is shown in Figure 5. Since the circuit configuration is identical for both modes, the same set of state equations and matrices applies.

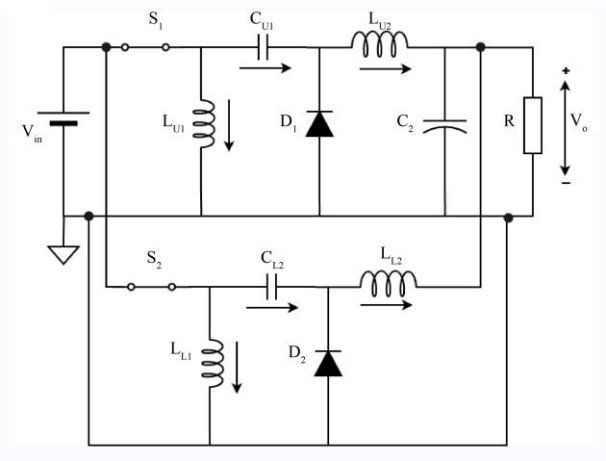

Fig. 5 Mode-1 & Mode-3 operation of IZ converter

In this interval, the inductors in both upper and lower phases are energized by the input source, causing their currents to increase linearly. The converter's differential equations are derived using Kirchhoff's voltage law (KVL) and Kirchhoff's current law (KCL), as listed in Table 2.

Table 2. Differential equations for Mode-1 and Mode-3 operation

During time $(0 < t < d_1T)$ and $(d_2T < t < d_3T)$ Switch S_1 ON and Switch S_2 ON	
$\frac{di_{LU1}}{dt} = \frac{V_{in}}{L_{U1}}$	$\frac{dV_{CU1}}{dt} = -\frac{i_{LU2}}{C_{u1}}$
$\frac{di_{LU2}}{dt} = \frac{V_{in}}{L_{U2}} + \frac{V_{CU1}}{L_{U2}} - \frac{V_{C2}}{L_{U2}}$	$\frac{dV_{CL1}}{dt} = -\frac{i_{LL2}}{C_{L1}}$
$\frac{di_{LL1}}{dt} = \frac{V_{in}}{L_{L1}}$	$\frac{dV_{C2}}{dt} = \frac{i_{LU2}}{C_2} + \frac{i_{LL2}}{C_2} - \frac{V_{C2}}{RC_2}$
$\frac{di_{LL2}}{dt} = \frac{V_{in}}{L_{L2}} + \frac{V_{CL1}}{L_{L2}} - \frac{V_{C2}}{L_{L2}}$	

From this set of differential equations, the state space matrices for Mode-1 and Mode-3 are obtained as:

$$A_1 = A_3 \begin{bmatrix} 0 & 0 & 0 & 0 & 0 & 0 & 0 \\ 0 & 0 & 0 & 0 & \frac{1}{L_{U2}} & 0 & \frac{-1}{L_{U2}} \\ 0 & 0 & 0 & 0 & 0 & 0 & 0 \\ 0 & 0 & 0 & 0 & 0 & \frac{1}{L_{L2}} & \frac{-1}{L_{L2}} \\ 0 & \frac{-1}{C_{U1}} & 0 & 0 & 0 & 0 & 0 \\ 0 & 0 & 0 & \frac{-1}{C_{L1}} & 0 & 0 & 0 \\ 0 & \frac{1}{C_2} & 0 & \frac{1}{C_2} & 0 & 0 & \frac{-1}{RC_2} \end{bmatrix}, \; B_1 = B_3 = \begin{bmatrix} \frac{1}{L_{U1}} \\ \frac{1}{L_{U2}} \\ \frac{1}{L_{L1}} \\ \frac{1}{L_{L2}} \\ 0 \\ 0 \\ 0 \end{bmatrix} \tag{11}$$

$$C_1 = C_3 = [0 \quad 0 \quad 0 \quad 0 \quad 0 \quad 0 \quad 1] \tag{12}$$

$$E_1 = E_3 = [0] \tag{13}$$

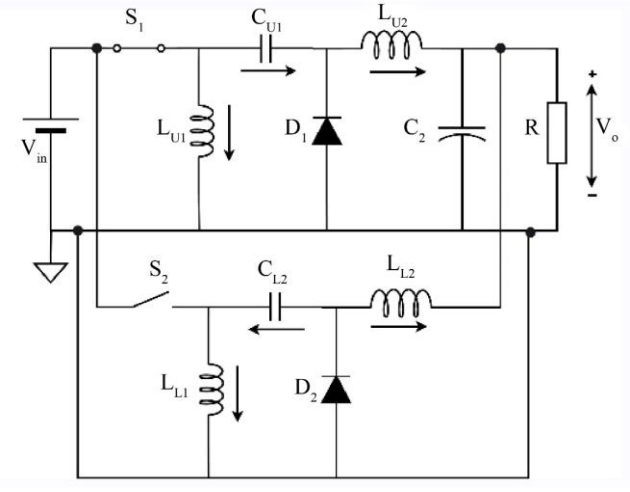

Fig. 6 Mode-2 operation of the Interleaved ZETA converter

4.4. Operation in Mode-2

For this mode of the IZ converter's operation, the switch in the upper phase is ON, while the switch in the lower phase is OFF. Corresponding diodes of each phase remain in opposite switching states with respect to the power switches. Figure 6 illustrates the Mode-2 operation of the converter. The currents i_{LU1} and i_{LU2} increase, while the inductor currents i_{LL1} and i_{LL2} decrease during this interval. During this period, the upper-phase inductors continue to store energy, while the lower-phase inductors deliver energy to the capacitors. In Table 3, the governing differential equations are listed.

Table 3. Differential equations for Mode-2 operation

During time $d_1T < t < d_2T$. Switch S_1 ON and Switch S_2 OFF	
$\frac{di_{LU1}}{dt} = \frac{V_{in}}{L_{U1}}$	$\frac{dV_{CU1}}{dt} = -\frac{i_{LU2}}{C_{u1}}$
$\frac{di_{LU2}}{dt} = \frac{V_{in}}{L_{U2}} + \frac{V_{CU1}}{L_{U2}} - \frac{V_{C2}}{L_{U2}}$	$\frac{dV_{CL1}}{dt} = \frac{i_{LL1}}{C_{L1}}$
$\frac{di_{LL1}}{dt} = -\frac{V_{CL1}}{L_{L1}}$	$\frac{dV_{C2}}{dt} = \frac{i_{LU2}}{C_2} + \frac{i_{LL2}}{C_2} - \frac{V_{C2}}{RC_2}$
$\frac{di_{LL2}}{dt} = -\frac{V_{C2}}{L_{L2}}$	

$$A_2 = \begin{bmatrix} 0 & 0 & 0 & 0 & 0 & 0 & 0 \\ 0 & 0 & 0 & 0 & \frac{1}{L_{U2}} & 0 & \frac{-1}{L_{U2}} \\ 0 & 0 & 0 & 0 & 0 & \frac{-1}{L_{L1}} & 0 \\ 0 & 0 & 0 & 0 & 0 & 0 & \frac{-1}{L_{L2}} \\ 0 & \frac{-1}{C_{U1}} & 0 & 0 & 0 & 0 & 0 \\ 0 & 0 & \frac{1}{C_{L1}} & 0 & 0 & 0 & 0 \\ 0 & \frac{1}{C_2} & 0 & \frac{1}{C_2} & 0 & 0 & \frac{-1}{RC_2} \end{bmatrix}, B_2 = \begin{bmatrix} \frac{1}{L_{U1}} \\ \frac{1}{L_{U2}} \\ 0 \\ 0 \\ 0 \\ 0 \\ 0 \end{bmatrix} \quad (14)$$

$$C_2 = [0 \quad 0 \quad 0 \quad 0 \quad 0 \quad 0 \quad 1] \quad (15)$$

$$E_2 = [0] \quad (16)$$

4.5. Operation in Mode-4

In Mode-4, the switch S_1 of phase 1 is in the OFF state, and the switch S_2 of phase 2 is in the ON state. In both phases, the corresponding diodes remain in complementary states with respect to the power switches.

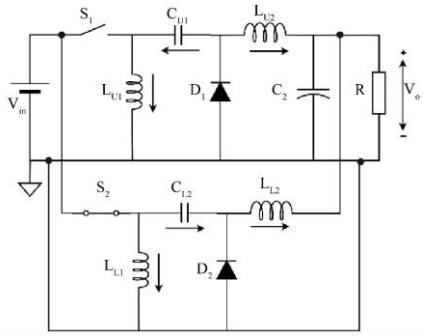

Fig. 7 Mode-4 operation of the Interleaved ZETA converter

$$A_4 = \begin{bmatrix} 0 & 0 & 0 & 0 & \frac{-1}{L_{U1}} & 0 & 0 \\ 0 & 0 & 0 & 0 & 0 & 0 & \frac{-1}{L_{U2}} \\ 0 & 0 & 0 & 0 & 0 & 0 & 0 \\ 0 & 0 & 0 & 0 & 0 & \frac{1}{L_{L2}} & \frac{-1}{L_{L2}} \\ \frac{1}{C_{U1}} & 0 & 0 & 0 & 0 & 0 & 0 \\ 0 & 0 & 0 & -\frac{1}{C_{L1}} & 0 & 0 & 0 \\ 0 & \frac{1}{C_2} & 0 & \frac{1}{C_2} & 0 & 0 & \frac{-1}{RC_2} \end{bmatrix}, \quad B_4 = \begin{bmatrix} 0 \\ 0 \\ \frac{1}{L_{L1}} \\ \frac{1}{L_{L2}} \\ 0 \\ 0 \\ 0 \end{bmatrix} \quad (17)$$

$$C_4 = [0 \quad 0 \quad 0 \quad 0 \quad 0 \quad 0 \quad 1] \quad (18)$$

$$E_4 = [0] \quad (19)$$

4.6. Average Modelling of the Interleaved ZETA Converter

To obtain the SSA augmented model of the IZ converter, the averaging of individual mode-wise state-space equations is performed for the whole switching interval. The switching sequence for *D>0.5* is illustrated in Figure 4, and the normalized time intervals are defined. For the overall converter operation within one switching cycle, the operating time of the individual phase can be determined from the switching pattern of the power switches. For duty cycle D, the normalized time intervals are defined as:

$$d_1 = \left(D - \frac{1}{2}\right) = d_3 \quad (20)$$

The corresponding circuit configuration is illustrated in Figure 7, indicating the direction of component currents. In this mode of operation, the lower-phase inductors are energized by the input source, and the upper-phase inductors release energy to the capacitors.

The resulting differential equations governing the converter dynamics are summarized in Table 4. The inductor currents i_{LU1} and i_{LU2} reduce, giving their energy to capacitors C_{U1} and C_2. Similarly, the inductor currents i_{LL1} and i_{LL2} rise linearly. The corresponding state space matrices are given as:

Table 4. Differential equations for Mode-4 operation

During time $d_3T < t < d_4T$. Switch S_1 OFF and Switch S_2 ON	
$\frac{di_{LU1}}{dt} = -\frac{V_{CU1}}{L_{U1}}$	$\frac{dV_{CU1}}{dt} = \frac{i_{LU1}}{C_{U1}}$
$\frac{di_{LU2}}{dt} = -\frac{V_{C2}}{L_{U2}}$	$\frac{dV_{CL1}}{dt} = -\frac{i_{LL2}}{C_{L1}}$
$\frac{di_{LL1}}{dt} = \frac{V_{in}}{L_{L1}}$	$\frac{dV_{C2}}{dt} = \frac{i_{LL2}}{C_2} + \frac{i_{LU2}}{C_2} - \frac{V_{C2}}{RC_2}$
$\frac{di_{LL2}}{dt} = \frac{V_{in}}{L_{L2}} + \frac{V_{CL1}}{L_{L2}} - \frac{V_{C2}}{L_{L2}}$	

$$d_2 = (1 - D) = d_4 \quad (21)$$

Where the addition of sub-intervals satisfies:

$$d_1 + d_2 + d_3 + d_4 = 1 \quad (22)$$

The averaged matrices can be derived as follows:

$$\begin{cases} A_T = d_1A_1 + d_2A_2 + d_3A_3 + d_4A_4 \\ B_T = d_1B_1 + d_2B_2 + d_3B_3 + d_4B_4 \\ C_{ST} = d_1C_{S1} + d_2C_{S2} + d_3C_{S3} + d_4C_{S4} \\ E_T = d_1E_1 + d_2E_2 + d_3E_3 + d_4E_4 \end{cases} \quad (23)$$

Using Equation 23,

From the averaged matrices of the converter, the transfer function is derived.

The converter transfer function is obtained for duty cycle values greater than 0.5 using Equation 8, and is expressed in the form:

$$G(s) = \frac{\text{Numerator Polynomial}}{\text{Denominator Polynomial}}$$

So, for duty cycle *D=0.5*,

$$G(s) = \frac{1.333e10\ s^5 + 0.001075\ s^4 + 3.788e16\ s^3 + 1581\ s^2 + 2.583e22\ s^1 + 1.24e08}{s^7 + 2.222e04\ s^6 + 1.387e08\ s^5 + 7.57e10\ s^4 + 3.059e14\ s^3 + 6.457e16\ s^2 + 1.291e20\ s^1 + 8.044e06} \quad (24)$$

The seventh-order transfer function of the interleaved topology is due to many energy-storing elements. The pole–zero characteristics indicate stable system behavior, which is further validated through the time-domain and frequency-domain responses presented in the following section.

5. Simulation Results

The converter's dynamic behavior is investigated using the developed SSA model. The MATLAB environment is employed to obtain the time and frequency-domain characteristics for a duty cycle greater than 0.5.

5.1. Time-Domain Response Analysis

Figure 8 depicts the time response of the output voltage under steady state and transient conditions for various duty cycles. The responses are captured using the SSA model, which indicates the dynamics of the converter.

The output voltage rises smoothly to steady state, with settling time varying approximately 0.016 sec to 0.03 sec based on duty cycle increase. The reduced settling time at higher duty cycle is due to increased energy transfer.

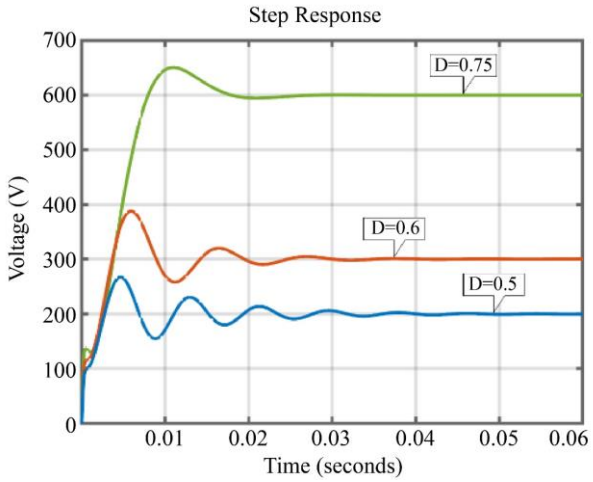

Fig. 8 Step response of IZ Converter

To validate the analytical model, the converter output responses obtained from the SSA model are matched with those obtained from the detailed Simulink circuit model using identical converter parameters. A close agreement between the two outcomes confirms the accuracy of the obtained SSA model in predicting dynamic behavior.

Table 5. Open-loop Poles and Zeros of the IZ converter

Poles	Complex P_1, P_2	(1.0e+04) x (–0.1015±0.2981i)
	Complex P_3, P_4	(1.0e+04) x (–0.0000 ± 0.1306i)
	Complex P_5, P_6	(1.0e+04) x (-0.0096 ± 0.0757i)
	At origin P_7	(1.0e+04) x (-0.0000+ 0.0000i)
Zeros	Complex Z_1, Z_2	(1.0e+03) x (-0.0000 ± 1.3056i)
	Complex Z_3, Z_4	(1.0e+03) x (0.0000 ± 1.0660i)
	At origin Z_5	(1.0e+03) x (-0.0000 + 0.0000i)

The poles and zeros are summarized in Table 5. The presence of seven poles and five zeros is compatible with the seventh-order dynamic model derived using the SSA technique.

5.2. Frequency-Domain Analysis

The converter's frequency-domain characteristics are analyzed using the small-signal transfer function derived as per Section 4. Figure 9 illustrates the magnitude and phase plots of the converter system for various duty cycles.

The Bode plot indicates that the open-loop system exhibits an infinite Gain Margin (GM) and a positive Phase Margin (PM), confirming inherent open-loop stability.

The captured frequency response provides valuable insight for the compensator design and closed-loop control in high-power applications, where dynamic performance and stability margins are most important.

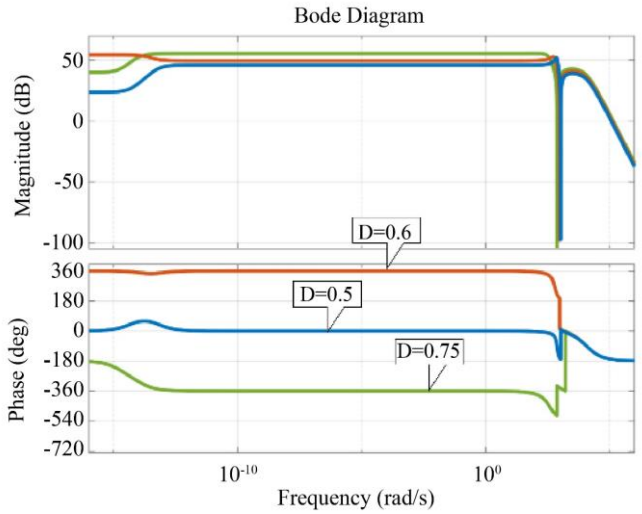

Fig. 9 Bode response of IZ Converter

5.3. Impulse Response Analysis

Figure 10 shows the converter impulse response for various duty cycles. The impulse response decays rapidly without sustained oscillations, indicating a well-damped system.

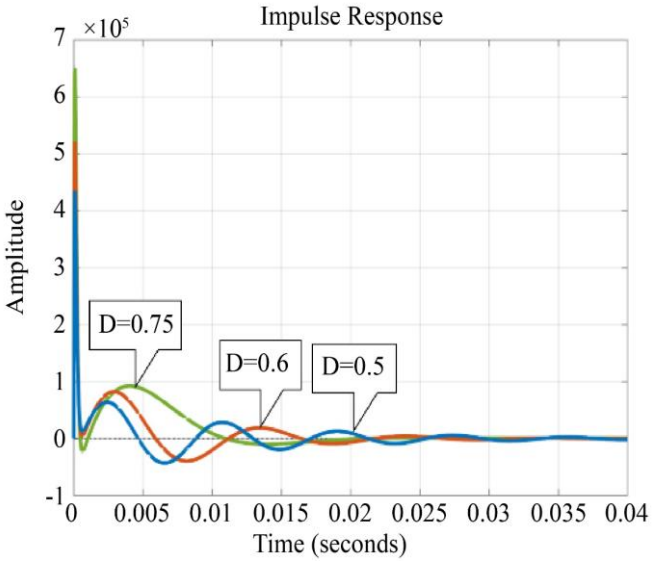

Fig. 10 Impulse response of IZ Converter

This behavior further confirms the stability of the interleaved ZETA converter and validates the correctness of the derived SSA model. The investigation of the impulse response is particularly useful for examining the inherent dynamic characteristics of the converter prior to the implementation of any feedback control strategy.

5.4. Discussion

The simulation results reveal that the developed SSA model accurately predicts the converter's dynamic characteristics over a range of duty cycles. The model is computationally efficient and well-suited for control-oriented analysis, enabling systematic controller design using classical or modern control techniques.

Based on the obtained SSA model of the converter, the step response and frequency domain parameters are evaluated, as summarized in Tables 6 and 7.

Table 6. Step input behavior of the IZ converter

Duty Cycle D	Settling time (sec)	Rise time (sec)	Overshoot (%)	Peak (V)
0.5	0.0340	0.0024	33.6810	267.355
0.6	0.0233	0.0032	29.1953	387.648
0.75	0.0159	0.0066	8.3517	650.078

Table 7. Bode plot Step input behavior of the IZ converter

Duty Cycle D	Gain Margin GM (dB)	Phase Margin PM (Degree)	Gain cross-over frequency Wcp (Hz)	Phase cross-over frequency Wcg (Hz)
0.5	Inf	10.164˚	1.063e+03	Not observed
0.6	Inf	10.081˚	1.26e+05	Not observed
0.75	Inf	9.014˚	1.41e+05	Not observed

The following points are examined from the obtained parameters,

- From the step response results presented in Table 6, the settling time decreases from 0.034 sec to 0.0159 sec with an increase in duty cycle, indicating faster system dynamics.
- The frequency domain characteristics listed in Table 7 show that the Gain Margin (GM) remains infinite, implying the absence of phase cross-over frequency.
- The phase margin is observed to lie between approximately 9° and 10°, indicating marginally stable open-loop behavior.

Decaying oscillations for all duty cycles in the impulse response show that the system is underdamped, stable, and has dominant complex conjugate poles.

In the literature, conventional studies on DC-DC converters primarily focus on basic topologies, which often rely on simulation-based analysis. The present work develops a systematic development of a state-space average model for a two-phase interleaved ZETA converter. In addition, although existing publications focus on performance improvement, little emphasis has been given to the

comprehensive dynamic analysis using the SSA technique. The proposed approach provides an accurate and structured representation of the converter dynamics.

6. Conclusion

This paper presents a comprehensive state-space averaged modelling approach for a two-phase interleaved ZETA DC-DC converter operating in continuous conduction mode. The complete large-signal model is systematically derived using mode-wise differential equations, and the corresponding SSA model is obtained for dynamic analysis. The developed state-space model accurately captures both converters' transient and steady-state behavior, as validated through MATLAB/Simulink simulations. Time-domain and frequency-domain responses confirm the inherent stability of the converter, as well as validate the effectiveness of the proposed modelling approach in predicting dynamic performance. The proposed SSA-based model provides a control-oriented analytical framework that can be effectively utilized for the design and implementation of closed-loop controllers in high-power applications. The developed model can be used in future studies towards the implementation and experimental assessment of advanced control strategies.

References

[1] Niraj Rana, and Subrata Banerjee, "Development of an Improved Input-Parallel Output-Series Buck-Boost Converter and Its Closed-Loop Control," *IEEE Transactions on Industrial Electronics*, vol. 67, no. 8, pp. 6428-6438, 2020. [CrossRef] [Google Scholar] [Publisher Link]

[2] Radha Kushwaha, and Bhim Singh, "An Electric Vehicle Battery Charger with Interleaved PFC Cuk Converter," *2018 8th IEEE India International Conference on Power Electronics (IICPE)*, Jaipur, India, pp. 1-6, 2018. [CrossRef] [Google Scholar] [Publisher Link]

[3] Peter Azer, and Ali Emadi, "Generalized State Space Average Model for Multi-Phase Interleaved Buck, Boost and Buck-Boost DC-DC Converters: Transient, Steady-State and Switching Dynamics," *IEEE Access*, vol. 8, pp. 77735-77745, 2020. [CrossRef] [Google Scholar] [Publisher Link]

[4] Radha Kushwaha, and Bhim Singh "Interleaved Landsman Converter Fed EV Battery Charger with Power Factor Correction," *IEEE Transactions on Industry Applications*, vol. 56, no. 4, pp. 4179-4192, 2020. [CrossRef] [Google Scholar] [Publisher Link]

[5] Phatiphat Thounthong, and Bernard Davat, "Study of a Multiphase Interleaved Step-up Converter for Fuel Cell High Power Applications," *Energy Conversion and Management*, vol. 51, no. 4, pp. 826-832, 2010. [CrossRef] [Google Scholar] [Publisher Link]

[6] B. Hu, and S. Sathiakumar, "A New Interleaving Technique Based on Current Ripple Reduction of Paralleled Converters for Renewable Systems," *Australian Journal of Electrical & Electronics Engineering*, vol. 11, no. 1, pp. 41-54, 2014. [CrossRef] [Google Scholar] [Publisher Link]

[7] Bor-Ren Lin, Po-Li Chen, and Jyun-Ji Chen, "Interleaved Sepic Converter with Low Switching Loss," *TENCON 2010 - 2010 IEEE Region 10 Conference*, Fukuoka, Japan, pp. 1817-1822, 2010. [CrossRef] [Google Scholar] [Publisher Link]

[8] Rodney H.G. Tan, and Landon Y. H. Hoo, "DC-DC Converter Modeling and Simulation using State Space Approach," *2015 IEEE Conference on Energy Conversion (CENCON)*, Johor Bahru, Malaysia, pp. 42-47, 2015. [CrossRef] [Google Scholar] [Publisher Link]

[9] Andressa C. Schittler et al., "Generalized State-space Model for the Interleaved Buck Converter," *IEEE XI Brazilian Power Electronics Conference*, Natal, Brazil, pp. 451-457, 2011. [CrossRef] [Google Scholar] [Publisher Link]

[10] T. Polsky et al., "Transient and Steady-State Analysis of a SEPIC Converter by an Average State-Space Modelling," *2018 IEEE 18th International Power Electronics and Motion Control Conference (PEMC)*, Budapest, Hungary, pp. 211-215, 2018. [CrossRef] [Google Scholar] [Publisher Link]

[11] Ricardo Aguilar-Najar et al., "Cascaded Buck Converter: A Reexamination," *2016 IEEE Transportation Electrification Conference and Expo (ITEC)*, Dearborn, MI, USA, pp. 1-5, 2016. [CrossRef] [Google Scholar] [Publisher Link]

[12] Ketsuda Karaket, and Chanin Bunlaksananusorn, "Modeling of a Quadratic Buck Converter," *The 8th Electrical Engineering/ Electronics, Computer, Telecommunications and Information Technology (ECTI) Association of Thailand - Conference 2011*, Khon Kaen, Thailand, pp. 764-767, 2011. [CrossRef] [Google Scholar] [Publisher Link]

[13] Mummadi Veerachary, and Shrikant Misal, "Single-switch Semi-Quadratic Buck Converter," *2020 IEEE International Conference on Power Electronics, Smart Grid and Renewable Energy (PESGRE2020)*, Cochin, India, 2020. [CrossRef] [Google Scholar] [Publisher Link]

[14] Folker Renken et al., "Multiphase DC/DC Converter and its Use in the Powertrain of Fuel Cell Vehicles," *2018 IEEE 18th International Power Electronics and Motion Control Conference (PEMC)*, Budapest, Hungary, pp. 280-286, 2018. [CrossRef] [Google Scholar] [Publisher Link]

[15] Kei Eguchi et al., "A Hybrid-Type High Step-Down DC/DC Converter Using a Step-Down Cross-Connected Fibonacci Converter," *2020 3rd International Conference on Power and Energy Applications (ICPEA)*, Busan, Korea (South), pp. 73-77, 2020. [CrossRef] [Google Scholar] [Publisher Link]

[16] Ioana-Monica Pop-Calimanu et al., "A Novel Hybrid Step-Down DC-DC Converter," *2018 IEEE 18th International Power Electronics and Motion Control Conference (PEMC)*, Budapest, Hungary, pp. 34-39, 2018. [CrossRef] [Google Scholar] [Publisher Link]

[17] Abdelsalam A. Ahmed et al., "New Interleaved-Input Double Float-Output DC/DC Converter Topology for Battery- Based EVs: Design, Modeling, Analysis and Experimental Implementation," *IEEE Access*, vol. 12, pp. 77870-77890, 2024. [CrossRef] [Google Scholar] [Publisher Link]

[18] Eladio Duran Aranda, Salvador Perez Litran, and Marıa Bella Ferrera Prieto, "Combination of Interleaved Single-input Multiple-output DC-DC Converters," *CSEE Journal of Power and Energy Systems*, vol. 8, no. 1, pp. 132-142, 2022. [CrossRef] [Google Scholar] [Publisher Link]

[19] M.T. Zhang, M.M. Jovanovic, and F.C.Y. Lee, "Analysis and Evaluation of Interleaving Techniques in Forward Converters," *IEEE Transactions on Power Electronics*, vol. 13, no. 4, pp. 690-698, 1998. [CrossRef] [Google Scholar] [Publisher Link]

[20] P.A. Dahono et al., "Output Ripple Analysis of Multiphase DC-DC Converters," *Proceedings of the IEEE 1999 International Conference on Power Electronics and Drive Systems. PEDS'99 (Cat. No.99TH8475)*, Hong Kong, China, vol. 2, pp. 626-631, 1999. [CrossRef] [Google Scholar] [Publisher Link]

[21] Padala Lakshmi Santosh Kumar Reddy et al., "A Non-Isolated Hybrid Zeta Converter with a High Voltage Gain and Reduced Size of Components," *Electronics*, vol. 11, no. 3, pp. 1-17, 2022. [CrossRef] [Google Scholar] [Publisher Link]

[22] C.T. Rim, G.B. Joung, and G.H. Cho, "A State-space Modeling of Nonideal DC-DC Converters," *PESC '88 Record., 19th Annual IEEE Power Electronics Specialists Conference*, Kyoto, Japan, vol. 2, pp. 943-950, 1988. [CrossRef] [Google Scholar] [Publisher Link]

[23] David Angulo-García, Fabiola Angulo, and Juan-Guillermo Muñoz, "DC-DC Zeta Power Converter: Ramp Compensation Control Design and Stability Analysis," *Applied Sciences*, vol. 11, no. 13, pp. 1-18, 2021. [CrossRef] [Google Scholar] [Publisher Link]

[24] Emerson Madrid et al., "Modelling of SEPIC, Cuk and Zeta Converters in Discontinuous Conduction Mode and Performance Evaluation," *Sensors*, vol. 21, no. 22, pp. 1-28, 2021. [CrossRef] [Google Scholar] [Publisher Link]